

2023-08

# Legacy radionuclides in cryoconite and proglacial sediment on Orwell Glacier, Signy Island, Antarctica

Owens, PN

<https://pearl.plymouth.ac.uk/handle/10026.1/21421>

---

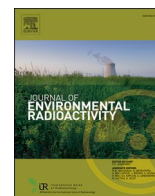
10.1016/j.jenvrad.2023.107206

Journal of Environmental Radioactivity

Elsevier BV

---

*All content in PEARL is protected by copyright law. Author manuscripts are made available in accordance with publisher policies. Please cite only the published version using the details provided on the item record or document. In the absence of an open licence (e.g. Creative Commons), permissions for further reuse of content should be sought from the publisher or author.*



## Legacy radionuclides in cryoconite and proglacial sediment on Orwell Glacier, Signy Island, Antarctica

Philip N. Owens<sup>a,\*</sup>, Tim A. Stott<sup>b</sup>, Will H. Blake<sup>c</sup>, Geoffrey E. Millward<sup>c</sup>

<sup>a</sup> Department of Geography, Earth and Environmental Sciences, and Quesnel River Research Centre, University of Northern British Columbia, Prince George, British Columbia, V2N4Z9, Canada

<sup>b</sup> School of Biological & Environmental Sciences, Faculty of Science, Liverpool John Moores University, Byrom Street Campus, Liverpool, L3 3AF, UK

<sup>c</sup> School of Geography, Earth and Environmental Sciences, University of Plymouth, Plymouth, PL4 8AA, UK

### ARTICLE INFO

#### Keywords:

Fallout radionuclides

Glacial retreat

Legacy contaminants

<sup>137</sup>Cs

Unsupported <sup>210</sup>Pb

### ABSTRACT

Cryoconite is a specific type of material found on the surface of glaciers and icesheets. Samples of cryoconite were collected from the Orwell Glacier and its moraines, together with suspended sediment from the proglacial stream on Signy Island, part of the South Orkney Islands, Antarctica. The activity concentrations of certain fallout radionuclides were determined in the cryoconite, moraine and suspended sediment, in addition to particle size composition and %C and %N. For cryoconite samples ( $n = 5$ ), mean activity concentrations ( $\pm 1SD$ ) of <sup>137</sup>Cs, <sup>210</sup>Pb<sub>un</sub> and <sup>241</sup>Am were  $13.2 \pm 20.9$ ,  $66.1 \pm 94.0$  and  $0.32 \pm 0.64$  Bq kg<sup>-1</sup>, respectively. Equivalent values for the moraine samples ( $n = 7$ ) were  $2.56 \pm 2.75$ ,  $14.78 \pm 12.44$  and  $<1.0$  Bq kg<sup>-1</sup>, respectively. For the composite suspended sediment sample, collected over 3 weeks in the ablation season, the values ( $\pm$  counting uncertainty) for <sup>137</sup>Cs, <sup>210</sup>Pb<sub>un</sub> and <sup>241</sup>Am were  $2.64 \pm 0.88$ ,  $49.2 \pm 11.9$  and  $<1.0$  Bq kg<sup>-1</sup>, respectively. Thus, fallout radionuclide activity concentrations were elevated in cryoconite relative to moraine and suspended sediment. In the case of <sup>40</sup>K, the highest value was for the suspended sediment ( $1423 \pm 166$  Bq kg<sup>-1</sup>). The fallout radionuclides in cryoconite were 1–2 orders of magnitude greater than values in soils collected from other locations in Antarctica. This work further demonstrates that cryoconite likely scavenges fallout radionuclides (dissolved and particulate) in glacial meltwater. In the case of <sup>40</sup>K, the greater value in suspended sediment implies a subglacial source. These results are amongst the relatively few that demonstrate the presence of fallout radionuclides in cryoconites at remote locations in the Southern Hemisphere. This work adds to the growing contention that elevated activities of fallout radionuclides, and other contaminants, in cryoconites are a global phenomenon and may be a risk to downstream terrestrial and aquatic ecosystems.

### 1. Introduction

There is growing concern associated with the release of legacy contaminants from a melting cryosphere on downstream ecosystems and for human health (Beard et al., 2022; Clason et al., 2023). However, a recent report by the Intergovernmental Panel on Climate Change (IPCC) on the cryosphere identified that a major research gap exists in our understanding of the fate of such legacy contaminants and called for more studies (IPCC, 2019). While the occurrence of fallout radionuclides (FRNs) in glacier-fed environments remains poorly understood in comparison to other atmospherically derived contaminants – such as metals and persistent organic pollutants (e.g., Blais et al., 2001; Bogdal et al., 2009; Schmid et al., 2011; Pavlova et al., 2016; Ferrario et al., 2017) –

an increasing number of studies have reported high activity levels of FRNs in cryoconite from glaciers, predominantly in the Northern Hemisphere. Regions examined include the European Alps (Tieber et al., 2009; Baccolo et al., 2017, 2020a, 2020b; Wilfinger et al., 2018), the Caucasus in Georgia (Łokas et al., 2018), Svalbard (Chmiel et al., 2009; Łokas et al., 2016, 2019), Sweden (Clason et al., 2021), Norway (Łokas et al., 2022), the Novaya Zemlya Archipelago in Russia (Miroshnikov et al., 2021), Greenland (Hasholt et al., 2000) and British Columbia, Canada (Owens et al., 2019).

Cryoconite is a specific type of sediment found on the surface of glaciers and icesheets. It is typically located in cryoconite holes and composed of minerogenic particles and organic material (Cook et al., 2016; Rozwalak et al., 2022). The minerogenic component of cryoconite

\* Corresponding author.

E-mail address: [philip.owens@unbc.ca](mailto:philip.owens@unbc.ca) (P.N. Owens).

<https://doi.org/10.1016/j.jenvrad.2023.107206>

Received 11 March 2023; Received in revised form 6 May 2023; Accepted 10 May 2023

Available online 22 May 2023

0265-931X/© 2023 The Authors. Published by Elsevier Ltd. This is an open access article under the CC BY-NC-ND license (<http://creativecommons.org/licenses/by-nc-nd/4.0/>).

is derived from a variety of sources including local moraines and talus, as well as atmospheric dust from distal deserts, volcanoes, and anthropogenic sources (e.g., agricultural topsoil, mines and construction sites), and possibly extra-terrestrial material (Cook et al., 2016; Owens, 2020; Rozwalak et al., 2022). The thermal properties of this minerogenic material, relative to the surrounding ice, cause the glacial ice below this material to melt, creating holes which eventually contain the minerogenic material and liquid water. These micro-environments become favourable conditions for algae, bacteria, extracellular polymeric substances and invertebrates, amongst others (Rozwalak et al., 2022). In recent years, large wildfires have provided an additional source of organic material (e.g., black carbon) to glacial surfaces and icesheets (Keegan et al., 2014; Aubry-Wake et al., 2022). As described above, the thermal properties of the combined dark minerogenic and organic components of cryoconite decreases the albedo of the glacier surface and promotes glacial melt and retreat (Takeuchi, 2002). In addition, given its fine-grained and organic-rich composition, cryoconite appears to accumulate FRNs, including those released during nuclear weapons testing and nuclear accidents, such as <sup>137</sup>Cs and <sup>241</sup>Am, as well as natural radionuclides, such as <sup>210</sup>Pb (Baccolo et al., 2017, 2020a, 2020b; Clason

et al., 2021).

While there are now several studies of FRN concentrations in cryoconite in the Northern Hemisphere, as described above, there is a dearth of information for the Southern Hemisphere. Surprisingly, given its large surface area, high proportion of ice, and high number of glaciers, almost no studies have measured FRN activities in cryoconite samples from Antarctica, including its surrounding islands, with Buda et al. (2020) being a rare exception. This partly stems from the considerable logistical and financial issues associated with collecting such samples and the bureaucratic problems of removing material from Antarctica for subsequent analysis. This paper adds to the sparse dataset of FRN activities in cryoconite samples from Antarctica. Specifically, the objectives were to: (i) determine if FRN activity concentrations were elevated in cryoconite relative to proglacial moraine and suspended sediment; and (ii) evaluate if glacier melt is releasing FRNs to the downstream proglacial zone.

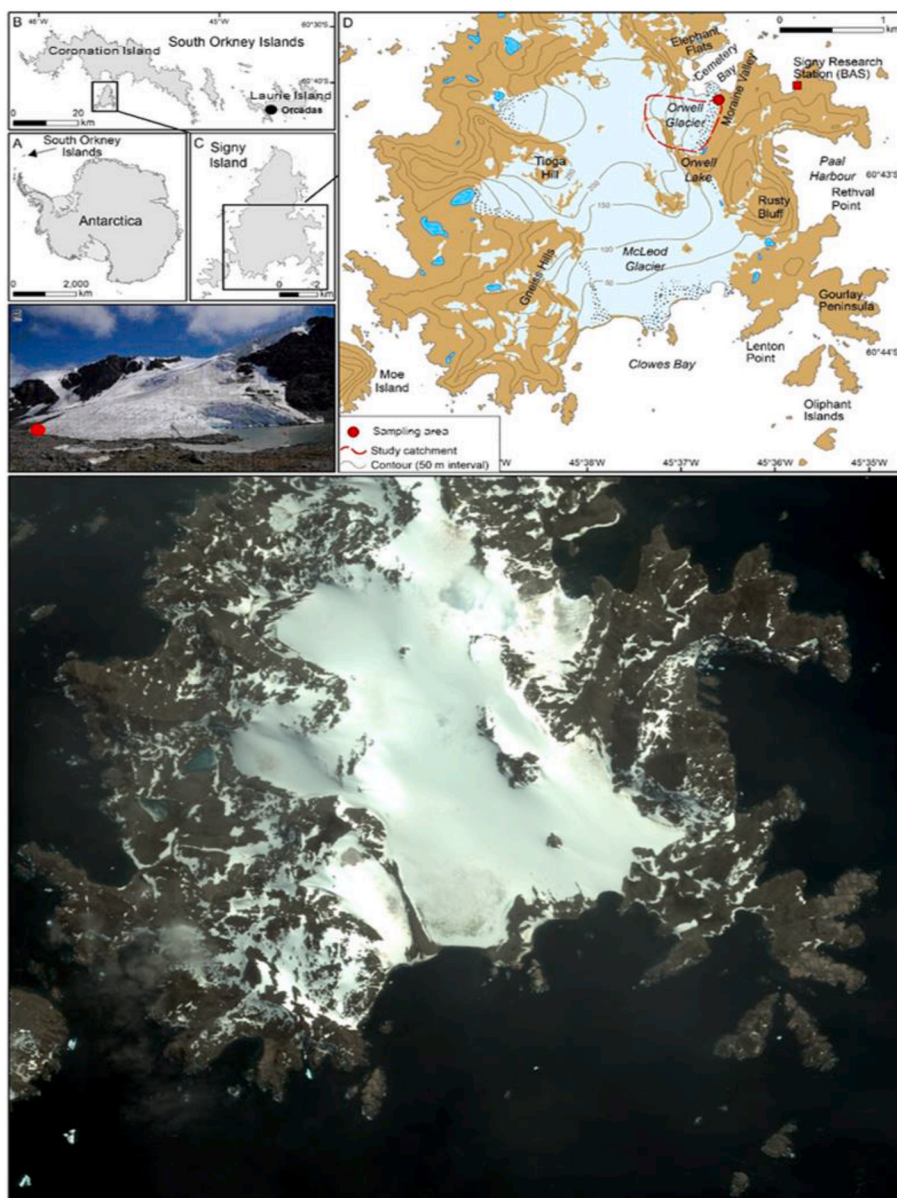


**Fig. 1.** Study location. A) The location of the South Orkney Islands in Antarctica. B) The South Orkney Islands showing the location of Signy Island. C) Signy Island with location of map insert (shown in D). D) The locations of Signy Research Station and the Orwell Glacier study catchment, with red dot showing the sampling location (see also photograph). The satellite image (bottom) taken in January 2010 was the most recent cloud-free image taken in summer. It covers the same area as the map in D and shows the Orwell Glacier margin and study site. (For interpretation of the references to colour in this figure legend, the reader is referred to the Web version of this article.)

## 2. Materials and methods

### 2.1. Study area

Signy Island (60°43'S, 45°38'W), in the maritime Antarctic South Orkney Islands (Fig. 1), has an area of 19 km<sup>2</sup> and is characterized by a cold oceanic climate. A research station has been maintained on the island since 1947, operated by the British Antarctic Survey (BAS, Fig. 1D). Signy Island's ice cap is shrinking rapidly, losing >1 m yr<sup>-1</sup> in thickness in recent decades (Favero-Longo et al., 2012). Permafrost is continuous, with an active layer thickness from 40 cm to >3 m (Guglielmin et al., 2008, 2012), which has recently been increasing by ~1 cm yr<sup>-1</sup> in response to increasing air temperatures (Cannone et al., 2006). Mean annual precipitation has been recorded at the Orcadas meteorological station at the nearby Laurie Island for >100 years (Fig. 1B) and is estimated to be ~400 mm yr<sup>-1</sup> for Signy Island (Stott and Convey, 2021). The bedrock is mainly quartz-mica-schist, although in some parts of the island there are small limestone outcrops (Matthews and Maling, 1967; Thomson, 1968; Guglielmin et al., 2012). The geomorphology of the island is characterized mainly by periglacial landforms and the hydrological and sedimentological characteristics of the sampling location are given in Stott and Convey (2021). This study focussed on Orwell Glacier, which is located on the north-east of the island, near the BAS field station (Fig. 1).

### 2.2. Sampling and analysis

#### 2.2.1. Field sampling

In January 2020, five cryoconite samples were collected from the surface of the glacier (OC1-OC5; Fig. 2) using a stainless-steel spatula; dry mass sample weights ranged from 371 to 457 g (mean 411 g). Samples were collected from the ablation zone of the glacier as this material is likely to be released to the proglacial zone given the rapid melt documented for this glacier, and allows for comparison with other studies that have normally collected cryoconite samples from this zone. While four of the samples can be considered as cryoconite (Cook et al., 2016; Rozwalak et al., 2022), one of the samples (OC5) was collected

from the surface of the glacier in an area that was covered by supra-glacial debris and represents a hybrid sample as it was a combination of supraglacial moraine and cryoconite material. The glacial samples were scraped from the ice and placed into clean zip-tie sample bags and sealed. In addition, seven samples of terminal moraine were collected within ca. 20 m of the glacial snout (OM1-OM7; Fig. 2) using the same technique but collecting material from the moraine surface to a depth of 2 cm; dry mass sample weights ranged from 439 to 534 g (mean 508 g). Both cryoconite and moraine samples were composites of several sub-samples collected within a surface area of ~1 m<sup>2</sup>. Water from the receiving proglacial river was collected over a 3-week period using plastic sample bottles which were emptied into an inert plastic box on five occasions until approximately 50 L was present. This was allowed to settle next to the stream for 7-days, after which the clear water was removed and a single 0.5 L sample of the concentrated suspended sediment-water mixture was retrieved for analysis. Samples were then sent via ship to the British Antarctic Survey, UK, for temporary storage and cataloguing before being sent to the Consolidated Radio-isotope Facility (CORiF; ISO9001) at the University of Plymouth, UK.

#### 2.2.2. Gamma spectroscopy

The sediment samples were prepared prior to performing FRN analyses following established protocols; the samples were dried, ground, homogenised and sieved both to <2 mm and also to <63 µm. The <2 mm fraction was used here as most other cryoconite studies (e.g., Tieber et al., 2009; Baccolo et al., 2017; Wilflinger et al., 2018) have analysed either the bulk (after removal of large particles and organic debris) or the <1 mm fraction. Thus the <2 mm fraction enables a more direct comparison with these other studies. This fraction also enables a direct comparison to other studies that have measured FRNs in soils in Antarctica (and is discussed later). The <63 µm fraction is the most mobile fraction and typically analysed in studies concerned with fluvial sediment quality and tracing in aquatic systems (Owens et al., 2016), and thus enables a more direct comparison between the mobile fraction of cryoconite and moraine samples and the suspended sediment sample. The <2 mm samples were packed and sealed in gas-tight Marinelli beakers (500 mL), while the <63 µm samples were packed and sealed in

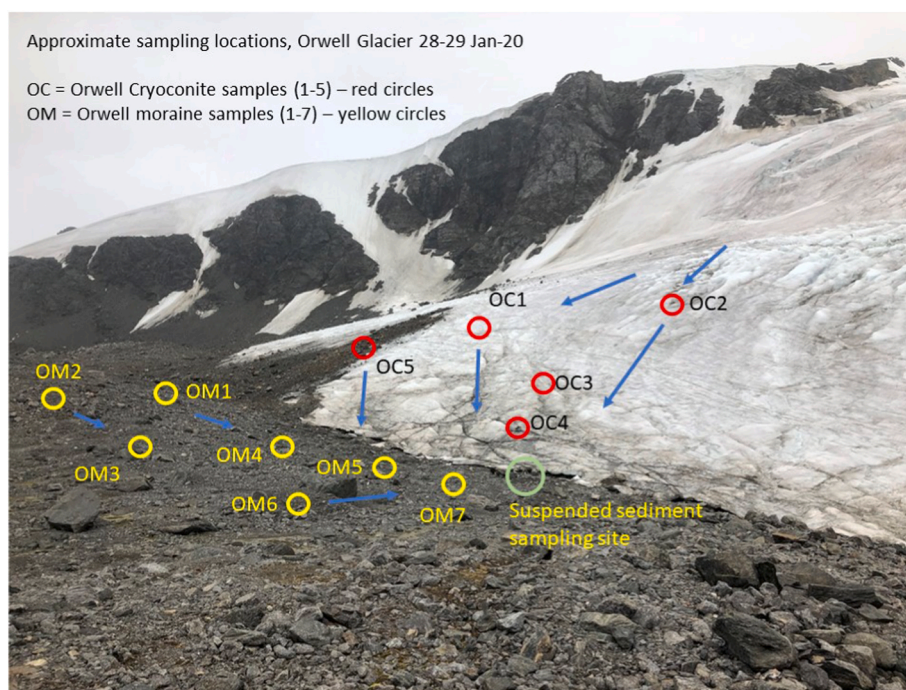


Fig. 2. Location of the cryoconite (OC1 – OC5) and moraine (OM1 – OM7) samples, and the site used to collect suspended sediment from the proglacial stream, Orwell Glacier.

aluminium gas-tight containers (130 mL) which had a similar diameter as the detector head. The sediment–water sample was centrifuged and the suspended solids were freeze-dried prior to packing in an aluminium gas-tight container. All packed samples were incubated for 21 days prior to counting to allow for the development of radioactive equilibrium.

Samples were analysed for FRNs using a hyper-pure germanium (HPGe) gamma spectrometry system (EG&G Ortec, UK; planar N-type detector; GMX50-83-LB-C-SMN-S). The system was calibrated using soil with a low background activity, spiked with a certified, traceable mixed radioactivity standard (80717-669 supplied by Eckert & Ziegler Analytics, Georgia, USA) of similar mass and the same geometry as the samples. All calibration relationships were derived using EG&G GammaVision software and verified by inter-laboratory comparison tests with materials supplied by the International Atomic Energy Agency (IAEA, e.g. IAEA-CU-2009-03; see Table SM1). The isotopes  $^{210}\text{Pb}$ ,  $^{241}\text{Am}$ ,  $^{214}\text{Pb}$  and  $^{137}\text{Cs}$  were determined from their gamma emissions at 46.5, 59.5, 295.3 (and 352.0) and 661.6 keV, respectively. Total  $^{210}\text{Pb}$  was measured and its unsupported component ( $^{210}\text{Pb}_{\text{un}}$ ) calculated by the subtraction of the  $^{226}\text{Ra}$  activity, which in turn was measured from the gamma emissions of  $^{214}\text{Pb}$ . Under certain circumstances, there can be issues associated with the self-absorption of gamma radiation by the sample mass, particularly for  $^{210}\text{Pb}$  gamma emission at 46 keV, which may require corrections (Jurian et al., 2018). Here, the mass of soil spiked with a radiologically certified liquid used in the calibrations was similar to the samples.

During analysis for the FRNs listed above, it became apparent that the activity concentrations for  $^{40}\text{K}$  – determined at 1460 keV as part of the routine analysis at CORiF – were higher for some samples than documented for other similar studies and thus  $^{40}\text{K}$  is also reported here. All activity concentrations were decay-corrected to 1 January 2021. Uncertainties, derived from the counting statistics, are reported as  $\pm 2$  sigma. The detection limits for the various radionuclides are dependent on the conditions of the gamma counting, and, under our analytical conditions, were approximately:  $^{241}\text{Am} < 1.0 \text{ Bq kg}^{-1}$ ;  $^{137}\text{Cs} < 1.0 \text{ Bq kg}^{-1}$ ;  $^{210}\text{Pb} < 5.0 \text{ Bq kg}^{-1}$ ;  $^{214}\text{Pb} < 2.0 \text{ Bq kg}^{-1}$  and  $^{40}\text{K} < 50 \text{ Bq kg}^{-1}$ .

### 2.2.3. Carbon, nitrogen and particle size

The analyses of total carbon (C) and nitrogen (N) were carried out combustionally using a Vario Micro Cube CHN analyser (Elementar<sup>®</sup>). The instrument was calibrated using acetanilide and each sample was determined in triplicate.

Prior to particle size analyses, the samples were digested in  $\text{H}_2\text{O}_2$  to remove organic matter and the wet samples were disaggregated in an ultrasonic bath. The particle size composition of the samples were determined using a laser optical particle-sizer (Mastersizer 2000; Malvern, UK) fitted with an auto-sampler and a Gradsat V8 statistical package. The samples were run in quintuplicate. The full dataset was checked for any large deviations from the mean distributions. The analytical errors for the dataset were  $< 5\%$  at the 95% confidence level.

### 2.3. Statistical analysis

Difference in properties (i.e., FRNs, particle size, %C, %N) between the various sample types (i.e., cryoconite and moraine) were assessed using the Mann-Whitney  $U$  test for unpaired samples, using a 95% probability of significance (i.e.,  $p = 0.05$ ). It is important to recognize that the low sample numbers ( $n = 5$  and  $7$ ) limits the statistical power of this test.

## 3. Results

### 3.1. Activity concentrations of $^{137}\text{Cs}$ , $^{210}\text{Pb}_{\text{un}}$ and $^{241}\text{Am}$

For the  $< 2 \text{ mm}$  fractions – here assumed to represent the bulk samples – activity concentrations of  $^{137}\text{Cs}$ ,  $^{210}\text{Pb}_{\text{un}}$  and  $^{241}\text{Am}$  in cryoconite were elevated relative to those in moraine sediments, although

none of these differences were statistically significant ( $p > 0.05$ ) due to the high variability (Fig. 3, Tables SM2 and SM3). For  $^{137}\text{Cs}$ ,  $^{210}\text{Pb}_{\text{un}}$  and  $^{241}\text{Am}$ , mean values ( $\pm 1\text{SD}$ ) were  $13.2 \pm 20.9$ ,  $66.1 \pm 94.0$  and  $0.32 \pm 0.64 \text{ Bq kg}^{-1}$ , respectively. Equivalent values for the moraine samples were  $2.56 \pm 2.75$ ,  $14.78 \pm 12.44$  and  $< 1.0 \text{ Bq kg}^{-1}$ , respectively. The highest values of the three FRNs were associated with OC1 ( $54.4$ ,  $249$  and  $1.6 \text{ Bq kg}^{-1}$  for  $^{137}\text{Cs}$ ,  $^{210}\text{Pb}_{\text{un}}$  and  $^{241}\text{Am}$ , respectively), followed by OC5, while values for the other three cryoconite samples fell within the range for moraine sediment. For the moraine samples, the highest values for  $^{137}\text{Cs}$  and  $^{210}\text{Pb}_{\text{un}}$  were measured in sample OM1; there was no  $^{241}\text{Am}$  detected in any of the moraine samples.

The single composite suspended sediment sample had activities for  $^{137}\text{Cs}$ ,  $^{210}\text{Pb}_{\text{un}}$  and  $^{241}\text{Am}$  of  $2.64 \pm 0.88$ ,  $49.2 \pm 11.9$  and  $< 1.0 \text{ Bq kg}^{-1}$ , respectively (Fig. 3). These were lower than equivalent values for the  $< 63 \mu\text{m}$  fraction of cryoconite of  $6.4 \pm 7.7$ ,  $87.1 \pm 75.4$  and  $0.25 \pm 0.50 \text{ Bq kg}^{-1}$ , respectively. The FRN activity concentrations for the suspended sediment sample were also lower than values for the  $< 63 \mu\text{m}$  fraction of the moraine samples (Fig. 3).

### 3.2. Activity concentrations of $^{40}\text{K}$

Similar to the other FRNs, the activity concentrations of  $^{40}\text{K}$  in the  $< 2 \text{ mm}$  fraction of cryoconite were elevated but not statistically different ( $p > 0.05$ ) from those in moraine samples (Fig. 3), with values of  $715 \pm 204$  and  $588 \pm 118 \text{ Bq kg}^{-1}$  for cryoconite and moraine, respectively. The activity concentration of the single composite suspended sediment sample was  $1423 \pm 166 \text{ Bq kg}^{-1}$  and this was noticeably greater than the average values for the  $< 63 \mu\text{m}$  fraction of cryoconite and moraine of  $967 \pm 302$  and  $1058 \pm 137 \text{ Bq kg}^{-1}$ , respectively.

### 3.3. Total carbon, nitrogen and particle size

The cryoconite samples analysed for FRNs had a statistically ( $p = 0.03$ ) greater proportion of material  $< 63 \mu\text{m}$  compared to the moraine samples;  $21.3 \pm 8.9\%$  vs  $10.1 \pm 5.3\%$ , respectively. Of the fraction  $< 63 \mu\text{m}$  (i.e., silts and clays), the median particle size ( $d_{50}$ ) was not statistically different for cryoconite and moraine samples;  $28.5 \pm 5.6$  and  $25.4 \pm 3.3 \mu\text{m}$ , respectively. The  $d_{50}$  for the single suspended sediment sample was  $15.7 \mu\text{m}$ .

In terms of %C and %N in the  $< 63 \mu\text{m}$  fractions, there were no statistical differences ( $p > 0.05$ ) between the two types of samples, with averages for C of  $0.30 \pm 0.09\%$  and  $0.29 \pm 0.04\%$  for cryoconite and moraine, and equivalent values for N of  $0.022 \pm 0.011$  and  $0.021 \pm 0.001\%$ , respectively. Values for the suspended sediment sample were  $0.23\%$  and  $0.04\%$  for C and N, respectively.

## 4. Discussion

### 4.1. Environmental radioactivity in the Northern and Southern Hemispheres

Environmental radioactivity due to artificial FRNs, such as  $^{137}\text{Cs}$  and  $^{241}\text{Am}$ , in the Southern Hemisphere originates primarily from two major sources. It is estimated that nuclear testing in the Southern Hemisphere from 1952 to 1974 resulted in a total of 2 Mt of fission products input into the troposphere, together with injection of 8 Mt of fission products into the stratosphere (Moroney, 1979). By comparison, from 1945 to 1979, atmospheric nuclear testing in the Northern Hemisphere produced 188 Mt of fission products of which 160 Mt was injected into the stratosphere. Consequently, fission products were transported from the Northern to the Southern Hemisphere at high altitude by seasonally driven zonal stratospheric air flows, ultimately resulting in additional fallout of long-lived radionuclides in the Southern Hemisphere. It has been estimated that these natural atmospheric processes resulted in the transport of 19–27 Mt of fission products from the north to south,

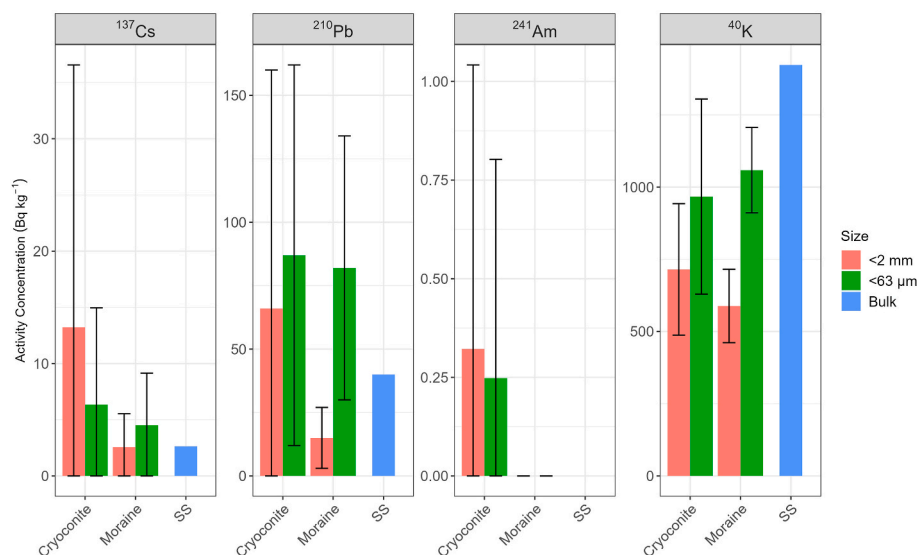


**Fig. 3.** Activity concentrations (mean  $\pm$ 1SD) of  $^{137}\text{Cs}$ ,  $^{210}\text{Pb}_{\text{un}}$ ,  $^{241}\text{Am}$  and  $^{40}\text{K}$  in cryoconite ( $n = 5$ ), moraine ( $n = 7$ ) and suspended sediment (SS;  $n = 1$ ) samples from Orwell Glacier. For cryoconite and moraine samples, concentrations are presented for the <2 mm and <63  $\mu\text{m}$  fractions.

thereby enhancing radionuclide deposition in the Southern Hemisphere. Thus, while the activities of FRNs in the Southern Hemisphere are generally low, the inter-hemispheric exchange of upper air masses has been instrumental in increasing the radionuclide contamination of the terrestrial environment of the Southern Hemisphere (Moroney, 1979).

The pattern described above is supported by Evrard et al. (2020) who estimated that  $\sim 2\%$  and  $\sim 1\%$  the total global fallout of  $^{137}\text{Cs}$  and  $^{210}\text{Pb}_{\text{un}}$  occurred between latitudes  $60^\circ$  and  $90^\circ$  S. In the case of  $^{137}\text{Cs}$ , this partly reflects the lower number of above-ground atom-bomb tests in the Southern Hemisphere, as described above, and the greater distance from major nuclear accidents and releases such as Chernobyl and Fukushima. Similarly, Zhang et al. (2021) report that the annual atmospheric deposition flux of  $^{210}\text{Pb}$  is two to three orders of magnitude lower in the latitudinal band  $60^\circ$  to  $90^\circ$  S than in  $20^\circ$  to  $50^\circ$  N; the latter coincides with the location of many of the cryoconite studies to date. Thus, it is expected that levels of many natural and artificial FRNs would be considerably lower in terrestrial materials in the Southern Hemisphere, especially towards the South Pole.

#### 4.2. Activity concentrations of $^{137}\text{Cs}$ , $^{210}\text{Pb}_{\text{un}}$ and $^{241}\text{Am}$ in cryoconite

Most studies to date have determined FRN activity concentrations in the bulk (i.e., no sieving) or <1 mm size fraction of cryoconite; here, the <2 mm fraction was used to enable comparison with these other studies. Although for a limited number of samples ( $n = 5$ ), FRN values for this size fraction for Orwell Glacier show considerable spatial variation, ranging over two orders of magnitude. The greatest values for  $^{137}\text{Cs}$  and  $^{210}\text{Pb}_{\text{un}}$ , and the only sample with measurable  $^{241}\text{Am}$  in the <2 mm fraction, were for OC1. Observations in the field suggest that this is the first site that was sampled to receive meltwater derived from further up the glacier (Fig. 2). Site OC5 had the next highest values for  $^{137}\text{Cs}$  and  $^{210}\text{Pb}_{\text{un}}$  ( $^{241}\text{Am} < \text{MDA}$ ) and is just below OC1. The other sites (OC2 to OC4) had lower FRN activity concentrations and were on steeper slopes, away from the main surface meltwater pathway. Previous studies (e.g., Baccolo et al., 2017, 2020a, 2020b; Owens et al., 2019) have postulated that cryoconite scavenges FRNs (dissolved and particulate) in passing meltwater. The concentrations of FRN in the meltwater, the amount of meltwater passing cryoconite, and the contact time between cryoconite and meltwater will all affect the FRN activity concentrations in the cryoconite and explain the large spatial variation observed at Orwell Glacier.

Furthermore, biogeochemical properties of the cryoconite holes,

such as total C and N content, are also likely to influence the scavenging potential of FRNs and stable elements. The values for %C and %N for Orwell Glacier (Section 3.3), although lower compared to many other studies of cryoconite (e.g., Cook et al., 2016), cohere well with values obtained in samples collected from cryoconite holes in three glaciers located in the Taylor Valley, Antarctica (Barrett et al., 2007). The low organic matter associate with samples from Antarctica may be due to the extreme cold and wind conditions. Fallout radionuclides are often more concentrated in finer and organic-rich soils and sediments (He and Walling, 1996). Indeed, the relation between FRN activity concentration and particle size and organic matter content has been demonstrated for cryoconite samples from other parts of the world (e.g., Owens et al., 2019). In the case of sample OC1, the <63  $\mu\text{m}$  fraction comprised 37% of the sample analysed (i.e., <2 mm), which compares to between 13 and 24% for samples OC2 to OC5. Thus, the fine nature of the cryoconite samples, especially OC1, partly explains the higher FRN activity concentrations compared to the moraine samples, which had statistically lower amounts of silts and clays (i.e., <63  $\mu\text{m}$  fraction). While the relation between FRN and organic matter content (i.e., %C) was less clear, sample OC5, which had the second highest levels of FRNs, had a noticeable greater %C (0.47%) compared to the other cryoconite and moraine samples (range: 0.21–0.38%). Thus, there is some evidence to suggest that the finer and more organic-rich cryoconite samples had the highest levels of FRNs, due to scavenging. However, a larger dataset would be required to provide more robust evidence.

The FRN activity concentrations for cryoconite from the Orwell Glacier in South Orkney Islands (Fig. 3) are lower than those measured in other parts of the world, which can be one to two orders of magnitude greater (see summary table in Owens et al., 2019). Thus, Clason et al. (2021) recorded average values ( $\pm$  counting error,  $n = 14$ ) of  $3069 \pm 941$ ,  $9777 \pm 780$  and  $25.8 \pm 16.7$  Bq  $\text{kg}^{-1}$  for  $^{137}\text{Cs}$ ,  $^{210}\text{Pb}_{\text{un}}$  and  $^{241}\text{Am}$ , respectively, for cryoconite samples from a small valley glacier in northern Sweden. As described above, in the case of  $^{137}\text{Cs}$  and  $^{210}\text{Pb}_{\text{un}}$ , the lower values measured in cryoconite samples from Orwell Glacier partly reflect the lower total fallout of these radionuclides in the Southern Hemisphere compared to the Northern Hemisphere. It may also reflect the relatively low organic matter content compared to those in samples collected from generally warmer locations in the Northern Hemisphere, where organic matter contents are typically between 5 and 20% (Cook et al., 2016).

Very few studies of FRN concentrations in cryoconite have been conducted in the Southern Hemisphere to enable comparison with those

from Orwell Glacier. For 10 cryoconite samples from Ecology Glacier on King George Island, Antarctica (675 km west of Signy Island), Buda et al. (2020) determined average activity concentrations of  $266 \pm 18$ ,  $1873 \pm 138$  and  $3.57 \pm 0.36$  Bq kg<sup>-1</sup> for <sup>137</sup>Cs, <sup>210</sup>Pb<sub>total</sub> and <sup>241</sup>Am, respectively. The reason for the higher FRN values for Ecology Glacier compared to Orwell Glacier is uncertain and may be due to several reasons, including differences in precipitation amounts (~500 vs ~400 mm year<sup>-1</sup>, respectively) and latitude (62° 11' vs 60° 43' S, respectively) (Buda et al., 2020; Stott and Convey, 2021), which partly control the amount of FRNs deposited of the Earth's surface. More likely, it is due to differences in the amount of melt in the ablation zone of the two glaciers and thus the contact of FRNs in surface runoff with cryoconite. Buda et al. (2020) report that glacial melt for the Ecology Glacier ranged from 1.7 m year<sup>-1</sup> (1979–2001) to 0.5 m year<sup>-1</sup> (2012–2016), while Favero-Longo et al. (2012) determined a decrease in thickness of >1 m year<sup>-1</sup> over several decades for Orwell Glacier. However, observations by Stott and Convey (2021) indicate that rates of melt at the snout at Orwell Glacier may be much greater in recent years. Clearly, the location of the cryoconite samples relative to surface runoff pathways is crucial in determining the amount of scavenging of FRNs by cryoconite. While it may be possible to determine such interactions under current conditions, this will have varied considerably over the lifespan of the FRNs examined here, and will be different for each FRN given differences in sources and deposition history. Further work is required to assess the mechanisms causing spatial variations in FRN activity concentrations of cryoconite both within and between glaciers.

Although no local soils were collected as part of this study, it is possible to compare the FRN activity concentrations of the cryoconite samples with topsoils from other studies conducted in Antarctica to assess the degree to which the cryoconite samples are elevated. These topsoils provide an indication of expected FRN activity concentrations of surface materials in the absence of glacial activity. Table 1 shows that FRN activity concentrations in topsoils are broadly consistent across sites, which cover a range of latitudes (~62° to 75° S). Compared to the cryoconite samples from the Orwell Glacier, for <sup>137</sup>Cs, <sup>210</sup>Pb<sub>un</sub> and

**Table 1**

Comparison of the FRN activity concentrations (Bq kg<sup>-1</sup>; mean ± 1 SD) in the cryoconite samples (<2 mm fraction) from Orwell Glacier with topsoils (typically 0–5 cm) collected from other locations in Antarctica. Where possible, FRNs have been decay-corrected to January 2021 to facilitate comparison with this study.

Location	Latitude	<sup>137</sup> Cs	<sup>210</sup> Pb <sub>un</sub>	<sup>241</sup> Am	<sup>40</sup> K	Source
Signy Island, South	60° 43' S	13.2 ±	66.1 ± 94.0	0.32 ± 0.64	715 ±	This study
Orkney Islands	45° 38' W	20.9			204	
King George and South Shetland Islands	62° 10' S	2.36 ±			240 ±	Godoy et al. (1998)
	58° 28' W	2.12			157	
Livingston Island, South Shetland Islands	62° 00' S	1.2 ± 1.1			317 ±	Navas et al. (2005)
	58° 00' W				227	
King George Island, South Shetland Islands	62° 13' S	5.3				Zhao et al. (2000)
	58° 58' W					
Terra Nova Bay, Antarctica	74° 18' S	~0.85	~5			Sbrignadello et al. (1994)
	165° 05' E					
Terra Nova Bay, Antarctica	74° 20' S	0.38 ±		0.006 ±		Jia et al. (2000)
	165° 07' E	0.32		0.005		

<sup>241</sup>Am they are 1–2 orders of magnitude lower, which confirms the elevated nature of FRNs in cryoconite. In the case of <sup>40</sup>K, values in topsoils are about half those in cryoconite.

#### 4.3. Activity concentrations of <sup>40</sup>K in cryoconite

Generally, activity concentrations for the primordial radionuclide <sup>40</sup>K have not been reported in most studies on cryoconite. The mean (±1SD) value for the <2 mm fraction of cryoconite samples from Orwell Glacier was  $715 \pm 204$  Bq kg<sup>-1</sup>. This value is higher than samples collected from the Blaisen Glacier in Norway ( $500 \pm 40$  Bq kg<sup>-1</sup>; Lokas et al., 2022) and similar to samples from the Forni (Italy) and Morteratsch (Switzerland) glaciers ( $770 \pm 200$  and  $810 \pm 55$  Bq kg<sup>-1</sup>, respectively; Baccolo et al., 2020a, 2020b). The <sup>40</sup>K activity concentrations for Orwell Glacier are lower than values for the Stubacher Sonnblöckes Glacier, Austria ( $1440 \pm 40$  Bq kg<sup>-1</sup>) and the Isfallsgläciären Glacier, Sweden ( $1839 \pm 168$  Bq kg<sup>-1</sup>, Clason et al., 2021). Given the limited information on <sup>40</sup>K – and many other radionuclides – in glacial environments, further studies are required.

#### 4.4. Comparison with FRNs in proglacial moraine and suspended sediment

For <sup>137</sup>Cs, <sup>210</sup>Pb<sub>un</sub> and <sup>241</sup>Am, the samples collected in the proglacial zone (moraine and suspended sediment) had lower values than the cryoconite. Although cryoconite material is likely to be supplied to the proglacial zone through melt of the glacier surface in the ablation season and glacial retreat over the last few decades (e.g., Lokas et al., 2017), the FRN signal is likely to be diluted by other sources of material such as subglacial sediment, atmospheric dust (local and regional), hillslopes and, in the case of the suspended sediment, from erosion of channel banks; all of which are likely to have lower activity concentrations of FRNs. Indeed, some of these sources, such as subglacial sediment, will only have received limited or, as in the case of <sup>137</sup>Cs and <sup>241</sup>Am, no fallout of radioactive material having been covered by tens to hundreds of metres of glacial ice until recently (Hasholt et al., 2000). This may partly explain the absence of <sup>241</sup>Am in the suspended sediment sample.

While the single suspended sediment sample – albeit an integrated sample collected over 3-weeks during the ablation season – is lower than the average FRN activity concentrations in cryoconite, for both <sup>137</sup>Cs and, especially, <sup>210</sup>Pb<sub>un</sub>, the values may also reflect the fact that the suspended sediment is finer than the cryoconite and moraine samples. This is due to particle size selectivity during sediment erosion and transport in the river channel due to hydrodynamic processes. Given the relation between <sup>137</sup>Cs and <sup>210</sup>Pb<sub>un</sub> concentrations and particle size (e.g., specific surface area), described above, then the suspended sediment may be preferentially enriched in these radionuclides compared to the original source. Furthermore, the finer stream particles may have an increased tendency for sorption of dissolved radionuclides.

For <sup>40</sup>K, the cryoconite and moraine samples were similar but the single suspended sediment was considerable greater. This suggests that the source of <sup>40</sup>K in suspended sediment is different than the other FRNs. The elevated value of <sup>40</sup>K relative to cryoconite and proglacial sediments may reflect weathering and glacial erosion of local bedrock and subglacial sediments from under the ice that is enriched in potassium, whereas this sediment source would not receive FRNs. This requires further investigation.

#### 4.5. Downstream impacts on terrestrial and aquatic ecosystems

Several studies have identified that the release of long-lived legacy contaminants such as FRNs may have detrimental impacts on downstream aquatic ecosystems and human health (IPCC, 2019; Owens et al., 2019; Clason et al., 2021, 2023; Beard et al., 2022). In many cases this is due to the close proximity of terrestrial and aquatic organisms and human populations to retreating glaciers, particular in parts of Asia,

Europe and North America. As the FRN activity concentrations associated with cryoconite, proglacial moraine and suspended sediment from Orwell Glacier are generally low, when compared to other studies, then this suggests that the immediate risk to downstream terrestrial and aquatic environments is low at present. For downstream areas where glacial water and sediment are focused, such as proglacial lakes and wetlands, then the ecosystem risk may be greater. Given the rapid retreat of Orwell Glacier and other glaciers in this area, then further monitoring and assessment are recommended.

## 5. Conclusions

Sediment samples from Orwell Glacier, South Orkney Islands, Antarctica, and suspended sediment from the downstream proglacial stream, had measureable activity concentrations of the long-lived FRNs  $^{137}\text{Cs}$ ,  $^{210}\text{Pb}$  and, in some cases,  $^{241}\text{Am}$ . The highest activities were found in the sediment collected from cryoconite holes and the dataset complements the emerging knowledge on the presence and concentrations of legacy contaminants, such as FRNs, in cryoconites in the Southern Hemisphere. The activity concentrations in cryoconite were, in some cases, orders of magnitude higher than those documented for topsoils in other Antarctic regions, confirming that they were elevated, in part due to glacial processes. The enriched activities of the FRNs illustrate the atmospheric fallout of radionuclides that were likely produced during the nuclear testing in the Southern Hemisphere which, over time, has been added to by fallout of radionuclides generated in the Northern Hemisphere and transported south via atmospheric inter-hemispheric transfer. While the FRN activity concentrations were lower in the suspended sediment compared to the cryoconite and moraine samples, suggesting that the downstream risk to terrestrial and aquatic ecosystems was minimal, the values for  $^{40}\text{K}$  were much higher. This suggests that the source of the  $^{40}\text{K}$  to the suspended sediment may be different than the other radionuclides, possibly from subglacial erosion of bedrock.

The radionuclide values from this geographically remote island add evidence to knowledge of the global distribution of cryoconites and their ability to scavenge radionuclides. It points to the need for further research on cryoconites, including their concentrations of FRNs and other contaminants, especially at isolated locations in the Southern Hemisphere, thereby allowing for inter-hemisphere comparisons.

## Declaration of competing interest

The authors declare that they have no known competing financial interests or personal relationships that could have appeared to influence the work reported in this paper.

## Data availability

Data will be made available on request.

## Acknowledgements

Matt Jobson, station leader of Signy Research Station, is thanked for logistical support, and Peter Convey (British Antarctic Survey, BAS) helped with gaining permission to take the samples and with their transport and handling at BAS. Samples were imported to the UK via DEFRA licence. Financial support was via the Natural Sciences and Engineering Research Council (NSERC; Discovery Grant RGPIN/6360–2018) of Canada. Laura Gerrish (BAS Mapping and Geographic Information Centre) and Kristen Kieta (UNBC) assisted with the preparation of the figures. The authors are grateful to Dr Martha Hall (CORiF Manager) for her assistance in the radiological analyses. Thanks are extended to the submission editor and two anonymous referees for constructive comments which helped to improve the paper.

## Appendix A. Supplementary data

Supplementary data to this article can be found online at <https://doi.org/10.1016/j.jenvrad.2023.107206>.

## References

- Aubry-Wake, C., Bertoncini, A., Pomeroy, J.W., 2022. Fire and ice: the impact of wildfire-affected albedo and irradiance on glacier melt. *Earth's Future* 10, e2022EF002685. <https://doi.org/10.1029/2022EF002685>.
- Baccolo, G., Di Mauro, B., Massabò, D., Clemenza, M., Nastasi, M., Delmonte, B., Prata, M., Prati, P., Previtali, E., Maggi, V., 2017. Cryoconite as a temporary sink for anthropogenic species stored in glaciers. *Sci. Rep.* 7, 9623. <https://doi.org/10.1038/s41598-017-10220-5>.
- Baccolo, G., Łokas, E., Gaca, P., Massabò, D., Ambrosini, R., Azzoni, R.S., Clason, C., Di Mauro, B., Franzetti, A., Nastasi, M., Prata, M., Prati, P., Previtali, E., Delmonte, B., Maggi, V., 2020a. Cryoconite: an efficient accumulator of radioactive fallout in glacial environments. *Cryosphere* 14, 657–672. <https://doi.org/10.1038/s41598-017-10220-5>.
- Baccolo, G., Nastasi, M., Massabò, D., Clason, C., Di Mauro, B., Di Stefano, E., Łokas, E., Priti, P., Previtali, E., Takeuchi, N., Delmonte, B., Maggi, V., 2020b. Artificial and natural radionuclides in cryoconite as tracers of supraglacial dynamics: insights from the Morteratsch glacier (Swiss Alps). *Catena* 191, 104577. <https://doi.org/10.1016/j.catena.2020.104577>.
- Barrett, J.E., Virginia, R.A., Lyons, W.B., McKnight, D., Priscu, J., Doran, P.T., Fountain, A., Wall, D.H., Moorhead, D.L., 2007. Biogeochemical stoichiometry of Antarctic dry valley ecosystems. *J. Geophys. Res.* 112, G01010. <https://doi.org/10.1029/2005JG000141>.
- Beard, D.B., Clason, C.C., Rangelroft, S., Poniacka, E., Ward, K.J., Blake, W.H., 2022. Anthropogenic contaminants in glacial environments II: release and downstream consequences. *Prog. Phys. Geogr.* 46, 630–648. <https://doi.org/10.1177/03091333221107376>.
- Blais, J.M., Schindler, D.W., Muir, D.C.G., Sharp, M., Donald, D., Lafreniere, M., Braekvelt, E., Strachan, W.M.J., 2001. Melting glacier dominate sources of persistent organochlorines to subalpine Bow Lake in Banff National Park. *Ambio* 30, 410–415. <https://doi.org/10.1579/0044-7447-30.7.410>.
- Bogdal, C., Schmid, P., Zennegg, M., Anselmetti, F.S., Scheringer, M., Hungerbühler, K., 2009. Blast from the past: melting glaciers as a relevant source for persistent organic pollutants. *Environ. Sci. Technol.* 43, 8173–8177. <https://doi.org/10.1021/es901628x>.
- Buda, J., Łokas, E., Pietryka, M., Richter, D., Magowski, W., Iakovenko, N., Porazinska, D.L., Budzik, T., Grabiec, M., Grzesiak, J., Klimaszuk, P., Gaca, P., Zawierucha, K., 2020. Biotope and biocenosis of cryoconite hole ecosystems on Ecology Glacier in the maritime Antarctic. *Sci. Total Environ.* 724, 138112. <https://doi.org/10.1016/j.scitotenv.2020.138112>.
- Cannone, N., Ellis-Evans, J.C., Strachan, R., Guglielmin, M., 2006. Interactions between climate, vegetation and active layer in maritime Antarctica. *Antarct. Sci.* 18, 323–333. <https://doi.org/10.1017/S0954-1020060037X>.
- Chmiel, S., Reszka, M., Rysiak, A., 2009. Heavy metals and radioactivity in environmental samples of the Scott Glacier region on Spitzbergen in summer 2005. *Quaest. Geogr.* 28A/1, 23–29.
- Clason, C.C., Blake, W.H., Selmes, N., Taylor, A., Boeckx, P., Kitch, J., Mills, S.C., Baccolo, G., Millward, G.E., 2021. Accumulation of legacy fallout radionuclides in cryoconite on Isfallsgläciären (Arctic Sweden) and their downstream spatial distribution. *Cryosphere* 15, 5151–5168. <https://doi.org/10.5194/tc-15-5151-2021>.
- Clason, C.C., Rangelroft, S., Owens, P.N., Łokas, E., Baccolo, G., Selmes, N., Beard, D., Kitch, J., Dextre, R.M., Morera, S., Blake, W., 2023. Contribution of glaciers to water, energy and food security in mountain regions: current perspectives and future priorities. *Ann. Glaciol.* <https://doi.org/10.1017/aog.2023.14>.
- Cook, J., Edwards, A., Takeuchi, N., Irvine-Fynn, T., 2016. Cryoconite: the dark biological secret of the cryosphere. *Prog. Phys. Geogr.* 40, 66–111. <https://doi.org/10.1177/0309133315616574>.
- Evrard, O., Chaboche, P.A., Ramon, R., Foucher, A., Lacey, J.P., 2020. A global review of sediment source fingerprinting research incorporating fallout radiocesium (Cs-137). *Geomorphology* 362, 107103. <https://doi.org/10.1016/j.geomorph.2020.107103>.
- Favero-Longo, S.E., Worland, M.R., Convey, P., Smith, R.I.L., Piervittori, R., Guglielmin, M., Cannone, N., 2012. Primary succession of lichen and bryophyte communities following glacial recession on Signy Island, South Orkney Islands, maritime Antarctic. *Antarct. Sci.* 24, 323–336. <https://doi.org/10.1017/S0954102012000120>.
- Ferrario, C., Finizio, A., Villa, S., 2017. Legacy and emerging contaminants in meltwater of three Alpine glaciers. *Sci. Total Environ.* 574, 350–357. <https://doi.org/10.1016/j.scitotenv.2016.09.067>.
- Godoy, J.M., Schuch, L.A., Nordemann, D.J.R., Reis, V.R.G., Ramalho, M., Recio, J.C., Brito, R.R.A., Olech, M.A., 1998.  $^{137}\text{Cs}$ ,  $^{226}$ ,  $^{228}\text{Ra}$ ,  $^{210}\text{Pb}$  and  $^{40}\text{K}$  concentrations in Antarctic soil, sediment and selected moss and lichen samples. *J. Environ. Radioact.* 41, 33–45. [https://doi.org/10.1016/S0265-931X\(97\)00084-2](https://doi.org/10.1016/S0265-931X(97)00084-2).
- Guglielmin, M., Ellis-Evans, J.C., Cannone, N., 2008. Active layer thermal regime under different vegetation conditions in permafrost areas. A case study at Signy Island (Maritime Antarctica). *Geoderma* 144, 73–85. <https://doi.org/10.1016/j.geoderma.2007.10.010>.
- Guglielmin, M., Worland, M.R., Cannone, N., 2012. Spatial and temporal variability of ground surface temperature and active layer thickness at the margin of maritime



- Antarctica., Signy Island. *Geomorphol.* 155, 20–33. <https://doi.org/10.1016/j.geomorph.2011.12.016>.
- Hasholt, B., Walling, D.E., Owens, P.N., 2000. Sedimentation in Arctic proglacial lake, Mittivakkat Glacier, south east Greenland. *Hydrol. Process.* 14, 679–699. [https://doi.org/10.1002/\(SICI\)1099-1085\(200003\)14:4<679::AID-HYP966>3.0.CO;2-E](https://doi.org/10.1002/(SICI)1099-1085(200003)14:4<679::AID-HYP966>3.0.CO;2-E).
- He, Q., Walling, D.E., 1996. Interpreting particle size effects in the adsorption of Cs-137 and unsupported Pb-210 by mineral soils and sediments. *J. Environ. Radioact.* 30, 117–137. [https://doi.org/10.1016/0265-931X\(96\)89275-7](https://doi.org/10.1016/0265-931X(96)89275-7).
- IPCC, 2019. IPCC special report on the ocean and cryosphere in a changing climate. In: Intergovernmental Panel on Climate Change. Cambridge University Press. <https://doi.org/10.1017/9781009157964>.
- Iurian, A.R., Millward, G.E., Sima, O., Taylor, A., Blake, W., 2018. Self-absorption for Pb-210 in gamma ray spectrometry using well and coaxial HPGe detectors. *Appl. Radiat. Isot.* 134, 151–156. <https://doi.org/10.1016/j.apradiso.2017.06.048>.
- Jia, G., Triulzi, C., Marzano, N., Belli, M., Vaghi, M., 2000. The fate of plutonium, <sup>241</sup>Am, <sup>90</sup>Sr and <sup>137</sup>Cs in the Antarctic ecosystem. *Antarct. Sci.* 12, 141–148. <https://doi.org/10.1017/S0954102000000183>.
- Keegan, K.M., Albert, M.R., McConnell, J.R., Baker, I., 2014. Climate change and forest fires synergistically drive widespread melt events of the Greenland ice sheet. *Proc. Natl. Acad. Sci. USA* 111, 7964–7967. <https://doi.org/10.1073/pnas.1405397111>.
- Lokas, E., Zaboraska, A., Koliccka, M., Rozycki, M., Zawierucha, K., 2016. Accumulation of atmospheric radionuclides and heavy metals in cryoconite holes on an Arctic glacier. *Chemosphere* 160, 162–172. <https://doi.org/10.1016/j.chemosphere.2016.06.051>.
- Lokas, E., Wachniew, P., Jodłowski, P., Gašiorel, M., 2017. Airborne radionuclides in the proglacial environment as indicators of sources and transfers of soil material. *J. Environ. Radioact.* 178–179, 193–202. <https://doi.org/10.1016/j.envrad.2017.08.018>.
- Lokas, E., Zawierucha, K., Cwanek, A., Szufa, K., Gaca, P., Mietelski, J.W., Tomankiewicz, E., 2018. The sources of high airborne radioactivity in cryoconite holes from the Caucasus (Georgia). *Sci. Rep.* 8, 10802 <https://doi.org/10.1038/s41598-018-29076-4>.
- Lokas, E., Zaboraska, A., Sobota, I., Gaca, P., Milton, J.A., Kocurek, P., Cwanek, A., 2019. Airborne radionuclides and heavy metals in high Arctic terrestrial environment as the indicators of sources and transfers of contamination. *Cryosphere* 13, 2075–2086. <https://doi.org/10.5194/tc-13-2075-2019>.
- Lokas, E., Wachniew, P., Baccolo, G., Gaca, P., Janko, K., Milton, A., Buda, J., Komędera, K., Zawierucha, K., 2022. Unveiling the extreme environmental radioactivity of cryoconite from a Norwegian glacier. *Sci. Total Environ.* 814, 152656 <https://doi.org/10.1016/j.scitotenv.2021.152656>.
- Matthews, D.H., Maling, D.H., 1967. *The Geology of the South Orkney Islands: I. Signy Island*, vol. 25. HMSO, London, p. 32.
- Miroshnikov, A., Flint, M., Asadulin, E., Aliev, R., Shiryayev, A., Kudikov, A., Khvostikov, V., 2021. Radioecological and geochemical peculiarities of cryoconite on Novaya Zemlya glaciers. *Sci. Rep.* 11, 23103 <https://doi.org/10.1038/s41598-021-02601-8>.
- Moroney, J.R., 1979. *Radioactive Fallout in the Southern Hemisphere from Nuclear Weapons Tests*. Australian Radiation Laboratory, p. 38. Report No. ARL/TR-013, ISSN 0157-1400.
- Navas, A., Soto, J., Lopez-Martinez, J., 2005. Radionuclides in soils of Byers Peninsula, south Shetland islands, western Antarctica. *Appl. Radiat. Isot.* 62, 809–816. <https://doi.org/10.1016/j.apradiso.2004.11.007>.
- Owens, P.N., 2020. Soil erosion and sediment dynamics in the Anthropocene: a review of human impacts during a period of rapid global environmental change. *J. Soils Sediments* 20, 4115–4143. <https://doi.org/10.1007/s11368-020-02815-9>.
- Owens, P.N., Blake, W.H., Gasper, L., Gateuille, D., Koiter, A.J., Lobb, D.A., Petticrew, E. L., Reiffarth, D.G., Smith, H.G., Woodward, J.C., 2016. Fingerprinting and tracing the sources of soils and sediments: Earth and oceans science, geoarchaeological, forensic, and human health applications. *Earth Sci. Rev.* 162, 1–23. <https://doi.org/10.1016/j.earscirev.2016.08.012>.
- Owens, P.N., Blake, W.H., Millward, G.E., 2019. Extreme levels of fallout radionuclides and other contaminants in glacial sediment (cryoconite) and implications for downstream aquatic ecosystems. *Sci. Rep.* 9, 12531 <https://doi.org/10.1038/s41598-019-48873-z>.
- Pavlova, P.A., Zennegg, M., Anselmetti, F.S., Schmid, P., Bogdal, C., Steinlin, C., Jaggi, M., Schwikowski, M., 2016. Release of PCBs from Silvretta glacier (Switzerland) investigated in lake sediments and meltwater. *Environ. Sci. Pollut. Res.* 23, 10308–10316. <https://doi.org/10.1007/s11356-015-5854-z>.
- Rozwalak, P., et al., 2022. Cryoconite – from minerals and organic matter to bioengineered sediments on glacier’s surfaces. *Sci. Total Environ.* 807, 150874. <https://doi.org/10.1016/j.scitotenv.2021.150874>.
- Sbrignadello, G., Degetto, S., Battiston, G.A., Gerbasì, R., 1994. Distribution of <sup>210</sup>Pb and <sup>137</sup>Cs in snow and soil samples from Antarctica. *Int. J. Environ. Anal. Chem.* 55, 235–242. <https://doi.org/10.1080/03067319408026221>.
- Schmid, P., Bogdal, C., Bluthgen, N., Anselmetti, F.S., Zwysig, A., Hungerbühler, K., 2011. The missing piece: sediment records in remote mountain lakes confirm glaciers being secondary sources of persistent organic pollutants. *Environ. Sci. Technol.* 45, 203–208. <https://doi.org/10.1021/es1028052>.
- Stott, T., Convey, P., 2021. Seasonal hydrological and suspended sediment transport dynamics and their future modelling in the Orwell Glacier proglacial stream, Signy Island, Antarctica. *Antarct. Sci.* 33, 192–212. <https://doi.org/10.1017/S0954102020000607>.
- Takeuchi, N., 2002. Optical properties of cryoconite (surface dust) on glaciers: the relationship between light absorbency and the property of organic matter contained in the cryoconite. *Ann. Glaciol.* 34, 409–414. <https://doi.org/10.3189/172756402781817743>.
- Thomson, J.E., 1968. *The geology of the South Orkney islands: II. In: The Petrology of Signy Island, vol. 62. British Antarctic Survey, Cambridge, p. 30.*
- Tieber, A., Lettner, H., Bossew, P., Hubmer, A., Sattler, B., Hofmann, W., 2009. Accumulation of anthropogenic radionuclides in cryoconites on Alpine glaciers. *J. Environ. Radioact.* 100, 590–598. <https://doi.org/10.1016/j.envrad.200904.008>.
- Wilflinger, T., Lettner, H., Hubmer, A., Bossew, P., Sattler, B., Slupetzky, H., 2018. Cryoconites from Alpine glaciers: radionuclide accumulation and age estimation with Pu and Cs isotopes and <sup>210</sup>Pb. *J. Environ. Radioact.* 186, 90–100. <https://doi.org/10.1016/j.jenvrad.2017.06.020>.
- Zhang, F., Wang, J., Baskaran, M., Zhong, Q., Wang, Y., Paatero, J., Du, J., 2021. A global dataset of atmospheric <sup>7</sup>Be and <sup>210</sup>Pb measurements: annual air concentration and deposition flux. *Earth Syst. Sci. Data* 13, 2963–2994. <https://doi.org/10.5194/eesd-13-2963-2021>.
- Zhao, Y., Li, T., Xu, C., 2000. The <sup>137</sup>Cs activity and its geographical significance in terrestrial ecosystem of Great Wall Station, Antarctica. *Chin. J. Polar Sci.* 11, 39–42.